UCLA
COMPUTATIONAL AND APPLIED MATHEMATICS

Two-Dimensional Boundary Layer Equations: High Resolution Capturing Schemes

Antonio Marquina

September 1991

CAM Report 91-18

Department of Mathematics
University of California, Los Angeles
Los Angeles, CA. 90024-1555

TWO-DIMENSIONAL BOUNDARY LAYER EQUATIONS: HIGH RESOLUTION CAPTURING SCHEMES

ANTONIO MARQUINA

September 12, 1991

Author's Current Address:
Antonio Marquina
Departamento de Matemática Aplicada
Universitat de València
C/ Dr. Moliner, 50
46100-Burjassot (Valencia) SPAIN
e-mail: marquinv@evalun11.bitnet
fax: (346)3864356

Two-Dimensional Boundary Layer Equations: High Resolution Capturing Methods

A. Marquina[1]

Departamento de Matemática Aplicada,
Universitat de València, 46100 Burjassot, Valencia, Spain

September 12, 1991

Abstract

In this paper we apply the piecewise hyperbolic and parabolic essentially non-oscillatory (ENO) capturing schemes (see [M91] and [SO89]) to approximate the solution to the boundary layer equations for two-dimensional incompressible flow. We have tested several numerical examples analyzing their resolutive power and efficiency with respect to small values of the kinematic viscosity of the flow.

L. Prandtl made a suitable simplification of the Navier-Stokes equations in order to describe the flow near the wall of a flat plate by dropping the equation of motion normal to the wall and reducing the unknowns by one, (from three to two). Indeed, if the wall is located at $y = 0$, u and v are the tangential and the normal components of the velocity, respectively, and ϵ is the kinematic viscosity, then we have the two-dimensional *Prandtl's boundary layer equations*

$$u_t + \left(\frac{u^2}{2}\right)_x + v \cdot u_y = -\frac{1}{\rho} \cdot p_x + \epsilon \cdot u_{yy} \tag{1.1}$$

$$u_x + v_y = 0, \tag{1.2}$$

[1]Research supported in part by a University of Valencia Grant and in part by a DARPA Grant in the ACM Program

where $0 \leq x, y \leq 1$, together with the initial tangential velocity profile

$$u(x, y, 0) = u_0(x, y), \tag{1.3}$$

and the boundary conditions

$$u(x, 0, t) = v(x, 0, t) = 0 \tag{1.4}$$

$$u(x, 1, t) = U(x, t) \tag{1.5}$$

where the potential flow $U(x, t)$ is to be considered known; it determines the pressure distribution with the aid of the equation

$$U_t + U \cdot U_x = -\frac{1}{\rho} \cdot p_x \tag{1.6}$$

where ρ is the density, (see [SCH]). The boundary layer thickness δ becomes proportional to $\sqrt{\epsilon}$ and the viscosity affects the flow essentially only in a very thin layer. The equation (1.1) is the equation of motion of the tangential velocity and equation (1.2) is the continuity equation. The boundary condition (1.4) means that the wall is at rest and if these values are settled to be a nonzero function then we would have a moving wall problem.

In this paper we have constructed two third order accurate capturing schemes to approximate the solution to the two-dimensional boundary layer equations. Both schemes have the same structure and they only differ on the reconstruction procedure used. We use either the piecewise hyperbolic or parabolic ENO reconstruction of numerical fluxes from the point values of the solution, in order to approximate the convective terms in (1.1). The viscosity term is approximated by means of a second order central difference, extrapolated up to fourth order accuracy. The scheme is designed as a method of lines and, therefore, the equation (1.1) can be integrated in time by means of an ODE (ordinary differential equation) solver. In our experiments we have used a total-variation diminishing, (TVD), third order Runge-Kutta method introduced by Shu and Osher in [SO88]. With this integration procedure our schemes become third order accurate in both space and time. The integration of the continuity equation (1.2) to recover v at every time level is performed at every time substep by means of an Euler forward scheme where the approximation of u_x is made through the third order accurate reconstruction procedure used for the convective terms of equation (1.1). Previously, TVD capturing schemes were used in [Y91] to solve some boundary layer problems and high order ENO schemes were applied to compressible free shear layers, (see [SEZWO91]).

We shall describe the scheme in some detail. We have used uniform grids. If Δx and Δy are the spatial stepsizes then we define the computational grid (x_i, y_j) for $i = 0, \cdots N$ and $j = 0, \cdots M$, where $x_i = i\,\Delta x$ and $y_j = j\,\Delta y$. We denote by Δt the time step and we define $t_l = l\,\Delta t$, for $l \geq 0$. We denote by $u^l_{i,j}$ and $v^l_{i,j}$ the approximation to the solution components $u(x_i, y_j, t_l)$ and $v(x_i, y_j, t_l)$, respectively. The one-stepping procedure is as follows. If we consider the following flux functions $f(u) := \frac{u^2}{2}$ and $g(u) := u$, then,

$$v^l_{i,j+1} = v^l_{i,j} - \frac{\Delta y}{\Delta x} \cdot (\hat{g}_{i+1/2,j} - \hat{g}_{i-1/2,j}) \tag{1.7}$$

$$u^{l+1}_{i,j} = u^l_{i,j} - \frac{\Delta t}{\Delta x} \cdot (\hat{f}_{i+1/2,j} - \hat{f}_{i-1/2,j}) -$$

$$- \frac{\Delta t}{\Delta y} \cdot v^l_{i,j} \cdot (\hat{g}_{i,j+1/2} - \hat{g}_{i,j-1/2}) + \Delta t \cdot (r_{i,j} + \epsilon \cdot s_{i,j}) \tag{1.8}$$

where $r_{i,j}$ is the term corresponding to the pressure gradient which is computed from the data and $s_{i,j}$ is the extrapolated second order central difference of $u's$ at (x_i, y_j). In order to be consistent with the boundary conditions it is necessary to integrate first the continuity equation, as it is showed in equation (1.7). Numerical fluxes are computed according to the direction of the wind and using the reconstruction procedure as defined either in [M91] in the hyperbolic case for nonlinear fluxes or in [SO89] in the parabolic one. The direction of the wind for the flux g in equation (1.8) is determined by the sign of $v^l_{i,j}$ through the y-direction. If there is a sonic point then a flux splitting is performed, (see [SO89] for details).

The one time-stepping procedure described before is *assumed* to be total variation stable for u, under a suitable CFL restriction of the form

$$\Delta t \cdot \left(\frac{\max|u|}{(\Delta x)^2} + \frac{\max|v|}{(\Delta y)^2} \right) \leq CFL \tag{1.9}$$

of parabolic type where CFL is called the Courant-Friedrichs-Lewy number. This stability cannot be proved neither for the hyperbolic method nor for the third order ENO, but there is some theoretical and numerical evidence to indicate these methods are indeed stable, (see [HEOC87] and [M91]).

The integration in time is made by means of the above mentioned Shu-Osher TVD third order Runge-Kutta method that is a convex combination of one time-stepping procedures described before.

We have tested several numerical examples in order to study the accuracy and stability of the scheme. Here, we will show what we consider as representatives. We denote by PHM the scheme designed from the hyperbolic reconstruction, (see [M91]) and by ENO3 the scheme designed by means of the parabolic ENO reconstruction, (see [SO89]).

The following features were found through our experiments:

1) We observed second order accuracy of the schemes at the boundary layer region for moving wall problems and the third order accuracy is recovered for problems where the wall is at rest. This accuracy is achieved when we have enough grid points to resolve the boundary layer and the number of grid points we need depends on the thickness of the layer.

2) When shocks appear PHM and ENO3 schemes behave in different ways. In order to be stable ENO3 scheme need a lower CFL number than the one necessary for the PHM. The PHM scheme is not sensitive to the CFL number, due to the fact that the hyperbolic reconstruction is more local than the parabolic one.

3) We remark that thanks to the fact that the convective terms are approximated in an upwind way, this allows us to use high CFL numbers, and according to our experiments the smaller kinematic viscosity we have, the larger CFL numbers can be chosen. Thus, the schemes become competitive concerning computational cost and CPU time.

Example 1 We consider the 2D boundary layer problem (1.1) and (1.2), with the initial tangential velocity profile

$$u(x,y,0) = \alpha + \beta \cdot (1-y) \cdot \sin(2\,\pi\,x - \gamma\,y) \tag{1.10}$$

u periodic in x with period 1 for every y, and the boundary conditions (1.4), and prescribing a potential flow $U(x,t) = \alpha$ for the outflow boundary $y = 1$. In order to study the accuracy of our schemes we have solved this problem for $\alpha = 1$, $\beta = 5$, $\gamma = 3$, $\epsilon = 0.03$ at $t = 0.05$ with $CFL = 16$, using both PHM and ENO3 schemes. The resolution for both schemes are similar and, then, we only show the 3D-plot and the level-plot for the PHM scheme and for a grid of 80×80 points, in figures 1 and 2, respectively. Let us observe a region of very large gradients interacting with the boundary layer region. In table 1 the L^∞- and L^1-errors are shown and they were computed at a slip of 2×20 computational grid, (where the boundary layer region is located), relative to the solution for a grid of 80×80. Richardson extrapolation shows

numerical evidence that the third order accuracy is recovered through this region.

Example 2 We consider the following example that is a simulation of a 2D boundary layer with moving wall, due to D. Gottlieb, (see [SO89], example 4),

$$u_t + \left(\frac{u^2}{2}\right)_x + u_y = \epsilon \cdot u_{yy} \tag{1.11}$$

where $0 \leq x, y \leq 1$, toghether with the initial tangential velocity profile

$$u(x, y, 0) = \alpha + \beta \cdot \sin(2\,\pi\, x) \tag{1.12}$$

and the boundary conditions

$$u(x, 0, t) = \alpha + \beta \cdot \sin(2\,\pi\, x) \tag{1.13}$$

u periodic in x with period 1. Since in this case we are supposed to know the normal velocity that is constant and equal to 1, it is not necessary to impose boundary conditions (i.e. a potential flow), at the outflow boundary. We have solved this problem for $\alpha = 0.5$, $\beta = 5$ and $\epsilon = 0.01$ at $t = 0.5$ with $CFL = 16$ for the same computational grids as for the example 1. In this case a shock has been developed and it is interacting with the boundary layer region generated at the moving wall $y = 0$. In table 2 the L^∞- and L^1-errors are shown and they were computed at a slip of 2×20 computational grid, (where the boundary layer region is located), relative to the solution for a grid of 80×80. We observe second order accuracy through this region.

According to the parameters used in both examples we have used the following formula to compute the time step satisfying (1.9):

$$\Delta t = \frac{CFL}{\left(\frac{7}{(\Delta x)^2} + \frac{1}{(\Delta y)^2}\right)} \tag{1.14}$$

Acknowledgements

I thank Stan Osher for suggesting the problem and for many helpful comments.

References

[HEOC87] A. Harten, B. Engquist, S. Osher and S. Chakravarthy, *Uniformly High Order Accurate Essentially Non-oscillatory Schemes III,* J. Comp. Phys. 71, 231 (1987)

[M91] A. Marquina, *Local Piecewise Hyperbolic Reconstruction of Numerical Fluxes for Nonlinear Scalar Conservation Laws,* UCLA CAM Report No. 89-25, (1989), SIAM J. Scient. Stat. Comp. (submitted).

[SO88] C.W. Shu, and S.J. Osher, *Efficient Implementation of Essentially Non-Oscillatory Shock-Capturing Schemes, I,* J. Comp. Phys. 77, 439 (1988)

[SO89] C. W. Shu and S.J. Osher, *Efficient Implementation of Essentially Non-Oscillatory Shock-Capturing Schemes, II,* J. Comp. Phys. 83, 32 (1989)

[SEZWO91] C. W. Shu, G. Erlebacher, T. Zang, D. Whitaker and S.J. Osher, *High-Order ENO Schemes Applied to Two- and Three-Dimensional Compressible Flow,* UCLA CAM Report 91-09, (1991)

[SCH] H. Schlichting "*Boundary-Layer Theory*" 7th. Ed. McGraw-Hill, N.Y. (1987)

[Y91] S. Yungster, *Numerical Study of Shock-Wave/Boundary Layer Interactions in Premixed Hydrogen-Air Hypersonic Flows,* NASA Technical Memorandum 103273, ICOMP-90-22, 19pp. (1991).

	L^∞-error		L^1-error	
$N \times M$	PHM	ENO3	PHM	ENO3
20×20	2.64	2.83	$2.50 \cdot 10^{-2}$	$2.50 \cdot 10^{-2}$
40×40	$4.62 \cdot 10^{-1}$	$4.60 \cdot 10^{-1}$	$4.08 \cdot 10^{-3}$	$3.90 \cdot 10^{-3}$

Table 1: **Wall at rest:** L^∞- and L^1-errors for 20×20 and 40×40 grid resolutions computed at the boundary layer region of 2×20 grid points

	L^∞-error		L^1-error	
$N \times M$	PHM	ENO3	PHM	ENO3
20×20	2.18	2.38	$4.90 \cdot 10^{-2}$	$5.10 \cdot 10^{-2}$
40×40	$6.34 \cdot 10^{-1}$	$6.73 \cdot 10^{-1}$	$1.73 \cdot 10^{-3}$	$1.79 \cdot 10^{-3}$

Table 2: **Moving Wall:** L^∞- and L^1-errors for 20×20 and 40×40 grid resolutions computed at the boundary layer region of 2×20 grid points

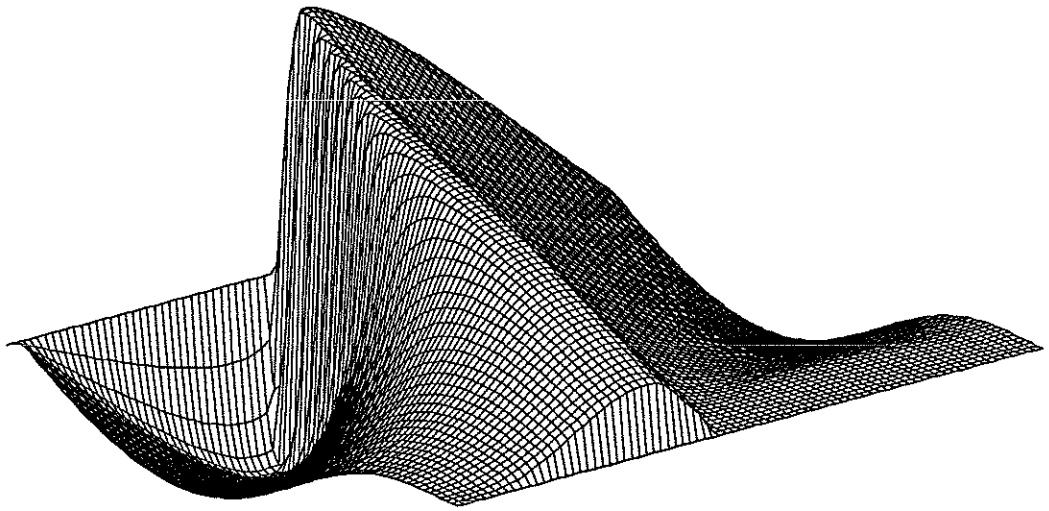

Figure 1: PHM, 80x80 grid points, CFL=16, t=0.05

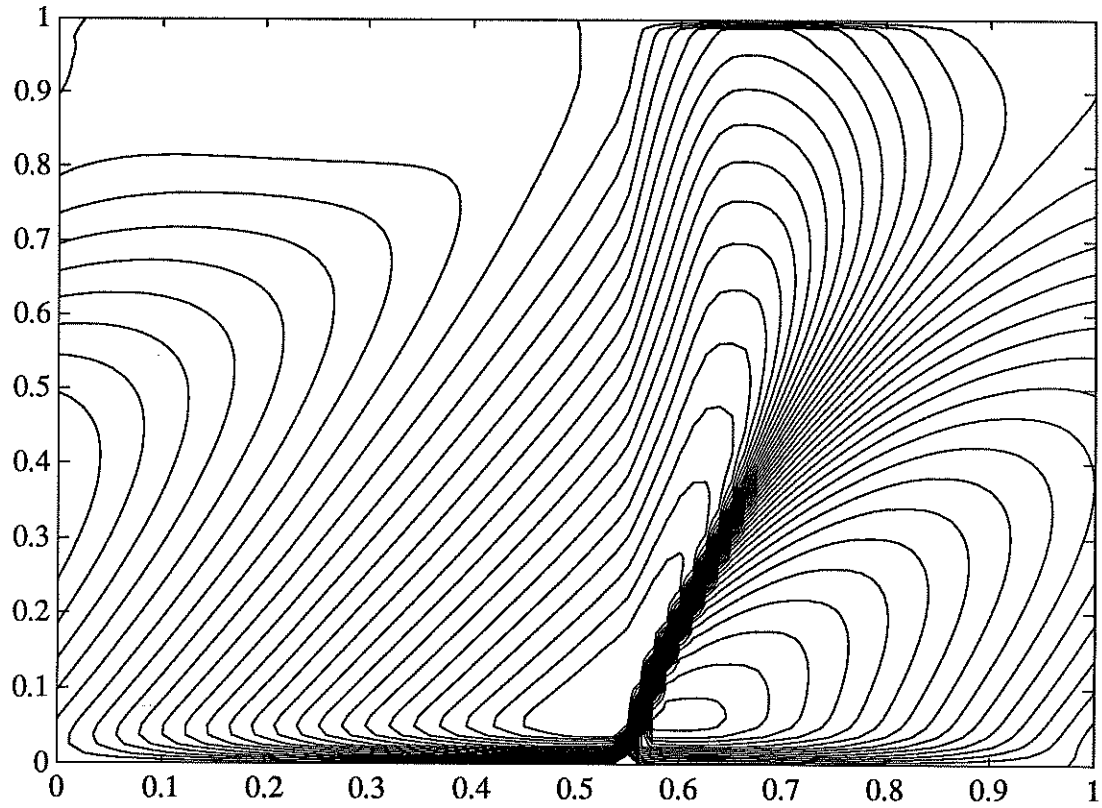

Figure 2: PHM, 80x80 grid points, CFL=16, t=0.05